Research Article

Eslam M. Hemid*, Tamás Kántor, Ahmed A. Tamma, and Mostafa A. Masoud*

Effect of groundwater fluctuation, construction, and retaining system on slope stability of Avas Hill in Hungary

https://doi.org/10.1515/geo-2020-0294
received July 12, 2021; accepted September 08, 2021

Abstract: Landslides are one of the natural hazards, which have significant negative effects on both humans and the environment. Thus, slope stability analyses and stabilization processes are necessary to obviate or mitigate landslides. In this study, the effect of groundwater level fluctuations and the construction of a building (i.e., a recently built church) on slope stability was investigated on the eastern slope of the Avas Hill, at Miskolc, in Northeast Hungary. Soil movements and groundwater levels were monitored and geological and slope stability models were constructed. Furthermore, the possibility of constructing a retaining system was evaluated to minimize the detrimental effects of both groundwater level fluctuations and the construction of the church. The findings showed that the fluctuation in groundwater levels had a destructive effect on slope stability due to pore-water pressure, which decreased the soil strength of the slope and slope stability. On the other hand, the church added an external load onto the underlying soil leading to an increase in slope instability. Hence, we suggested constructing retaining structures such as gravity retaining walls to increase the soil shear strength and enhance slope stability in the long term.

*** Corresponding author: Eslam M. Hemid,** Institute of Mineralogy and Geology, Faculty of Earth Science and Engineering, University of Miskolc, Miskolc-Egyetemváros, 3515, Hungary; Geology Department, Faculty of Science, Beni-Suef University, Beni Suef City, 62511, Egypt, e-mail: eslam.mohamed@science.bsu.edu.eg
*** Corresponding author: Mostafa A. Masoud,** Geology Department, Faculty of Science, Beni-Suef University, Beni Suef City, 62511, Egypt, e-mail: mostafa_masoud@science.bsu.edu.eg
Tamás Kántor, Ahmed A. Tamma: Department of Hydrogeology and Engineering Geology, Institute of Environmental Management, Faculty of Earth Science and Engineering, University of Miskolc, Miskolc-Egyetemváros, 3515, Hungary

Keywords: landslide, groundwater fluctuation, construction influence, slope stability, GEO5 program, golden software surfer

1 Introduction

Natural hazards, such as landslides, volcanic eruptions, floods, and earthquakes, are natural phenomena that occur without any human interference. They have significant negative effects on both humans and the environment as well. Landslides, which are defined as mass rock, debris, and slope processes are the most common natural hazard in mountainous regions [1]. In the last few years, many disasters resulting in thousands of deaths, injuries, and economic losses were caused by landslides [2]. They occur when a part of the natural slope becomes unstable, and moves when it fails to carry its weight. Therefore, it is imperative to investigate slope stability for interpreting the landslide mechanism, and to avoid its occurrence. Many factors govern the stability of a slope. They can be categorized into two main groups: natural and artificial factors [3,4]. One of the natural triggering factors is water, which is represented by variations in groundwater levels [5], snowmelt [6], or heavy rainfall [7]. The groundwater level plays a significant role in the evaluation and interpretation of landslide stability. Numerous landslide studies have revealed that water affects slope stability [8–11]: increasing groundwater levels and consequently increasing pore water pressure, groundwater exfiltration, uplifting due to hydraulic pressure, and the effect of water on landslide plasticity are ways in which water affects slope stability. The artificial factor is extensively represented by anthropogenic interactions, which are related to increased population, plantation, deforestation, quarrying, mining, and construction activities as a result of growing urbanization [12,13]. Then, the removal of deep-rooted vegetation binding colluviums to the bedrock followed by construction processes on the slopes are

the principal manmade factors threatening landslide stability. Root fibers increase the shear strength of the soil reducing slope deformation [14,15]. Additionally, these roots also reduce rainwater infiltration and delay the rising of the groundwater table [18].

Hence, many soil improvement and stabilization processes were suggested to avert or mitigate this hazardous phenomenon by increasing the strength of the soil. These stabilizing techniques can be mechanical [19,20], chemical [21–24], or biological [17,25–27]. Additionally, structural techniques such as retaining systems [28,29], stabilizing piles [30], and drainage tunnels [31] are used to mitigate soil instability.

Retaining systems are one of the common structural techniques to enhance soil stability [32,33]; they can hold back and strengthen the soil that has a problem in consolidation. These systems consist of a retaining wall constructed to retain the vertical or slightly vertical banks of earth materials or any other material. There are many types of retaining walls such as gravity walls, cantilever walls, fort-counter walls, anchors walls, and piled walls.

Hungary is a country that faces the threat of landslides [34]. The Avas Hill in the Northeast of Hungary is an area where plenty of landslides occur. Several landslides have occurred here earlier. Soil movements continue now too in this area [35], particularly, in the Northeast of the Bükk Mountains, at Miskolc, which also is the case study area of this project (Figure 1). In the last decades, as a result of landslides, soil movements were detected in Avas Hill with less than 2.5 mm/year displacement negatively affecting the upper part of the soil [36,37]. Although this displacement rate may not be enough to constitute a danger, any higher levels of surface movement could trigger landslides and endanger surrounding buildings. Recently, the landslides in Avas Hill have caused large fractures and joints in some buildings. They have also tilted trees and fences. However, the effects of groundwater, construction, and retaining systems on slope stability in this area have not been discussed earlier in any study. Hence, this study aims to comprehensively investigate the effects of groundwater fluctuations (natural factor) and constructing processes (artificial factor) on the slope stability of Avas Hill, at Miskolc, in the Northeast of Hungary. Moreover, we seek to reduce the soil movement effect and thereby increase slope stability by constructing gravity-retaining walls. For this purpose, the following approaches were taken: (1) monitoring the levels of groundwater in wells and the rate of soil displacement; (2) evaluation of slope stability on a finite slope using GEO5 software; and (3) evaluation of groundwater fluctuations, constructions, and the effect of retaining systems on slope stability using GEO5 software.

1.1 Location and climate

The study area is located between latitudes 48° 05′ 03″ N and 48° 5', 15″ N and longitudes 20° 46′ 31″ E and 20° 47′

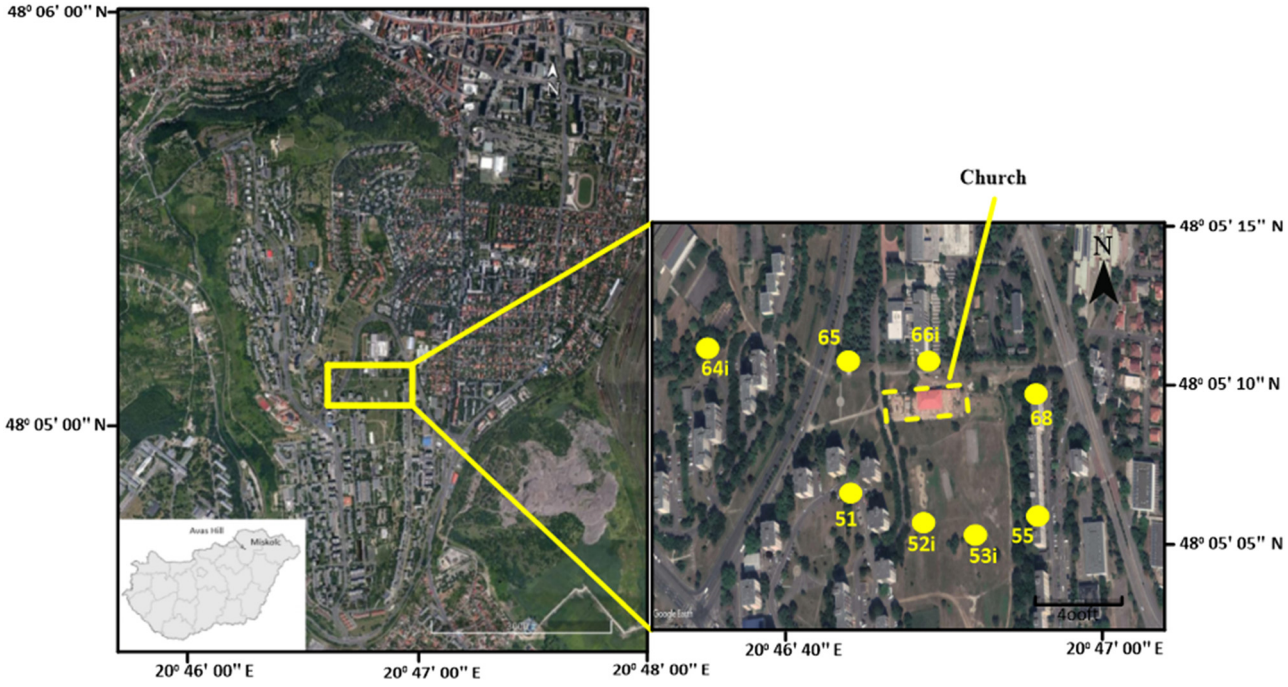

Figure 1: The map view of Avas Hill. The yellow circles represent the observation wells of the fifth and sixth lines.

05″ E (Figure 1). It is part of the Avas Hill, at Miskolc city, in Northeast Hungary, which was studied geologically, hydrogeologically, and geotechnically earlier [35]. It lies 124 m above sea level. The climate of Miskolc is classified as temperate and warm. The rate of rainfall in Miskolc is remarkable, as precipitation has occurred during the driest month as well. The average annual precipitation is about 551 mm/year. The maximum amount of rainfall occurs in July with an average of 83 mm; otherwise, the minimum amount of rainfall occurs in January with an average of 26 mm. Figure 1 shows eight observation wells (51, 52i, 53i, 55, 64i, 65, 66i, 68), which were used to measure the changes in soil displacements and groundwater fluctuation. Wells of 51, 52i, 53i, and 55 belong to the fifth line, while 64i, 65, 66i, and 68 wells are related to the sixth line.

1.2 Geological setting

Generally, Avas Hill's basement consists of Mesozoic rocks (Middle–Upper Triassic Bükkfennsík limestone), which are known here only from boreholes with a depth of about −100 to −200 m (Figure 2). This limestone is subjected to strong faulting and folding tectonics, which appears most prominently in the central part of the Bükk Mountains [38,39].

The Triassic limestone is covered with angular unconformity by Karpatian (upper part of the Lower Miocene) brackish and shallow marine deposits after a long weathering and erosion period. These deposits are clayey, silty, and sandy beds intercalated by thin layers of rhyolitic tuff, tuffite, and brown coal (Salgótarján Formation). The thickness of the Carpathian deposits ranges between 50 and 100 m. These deposits outcrop only on the western side of the Avas Hill. The Avas main mass, which overlain the Karpatian deposits, is built up of Middle Miocene (Badenian–Sarmatian) rhyolitic pyroclasts mixed with clastic sediments or pure volcanic material (Sajóvölgy Formation). This formation has a thickness between 55 and 100 m. The dip angle of layers is between 5 and 12 degrees toward S and SE. Sajóvölgy Formation's lower part consists of rhyolitic tuffs, while the upper part consists of highly variable beds of mostly andesitic tuff. The depositional and structural character of the andesitic

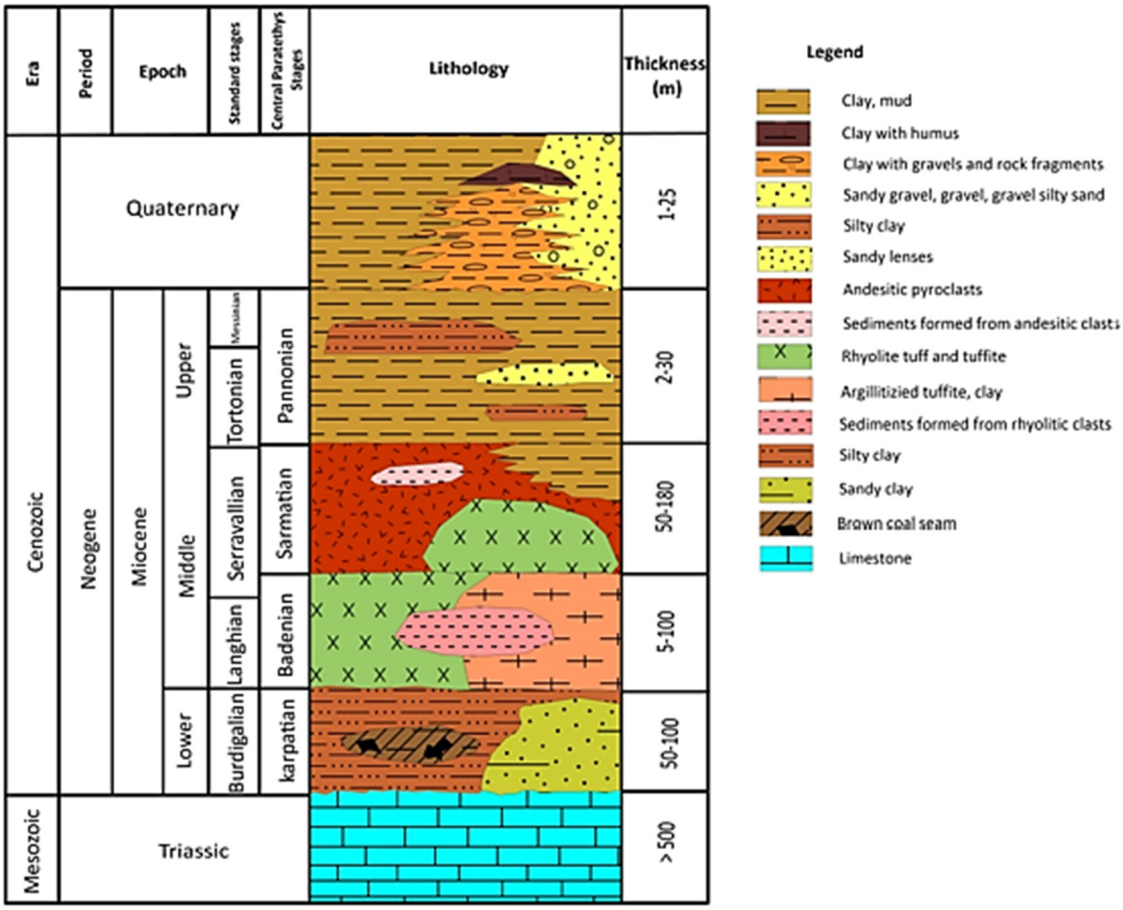

Figure 2: Geological section of Avas Hill (modified after refs [41,42]).

sequence indicates that it was formed mainly in the continental (terrestrial, lacustrine, and fluvial) environment based on the presence of flora (*Acer trilobatum* [Brongt.], *Carpinus grandis* [Ung.], *Phragmites oeningensis* [Brongt.], and *Salix varians* [Göpp.]) in the andesitic tuffs [40].

The Sajóvölgy Formation is overlaid by Pannonian deposits (Edelény Formation), which were only found in artificial exposures and drill holes. The thickness of the Pannonian deposits ranges between 2 and 30 m. The paleoenvironment of the Pannonian sequence was lacustrine, and fluvial, as indicated by the clayey–silty lithofacies and cross-bedded lenses in the sand, respectively [40]. Quaternary rocks cover the Pannonian sequence with 1–25 m in thickness. They are composed of aeolian and fluvial deposits, which originated from the weathering process of the andesitic tuffs (the upper part of Sajóvölgy Formation). Moreover, clastic sediments such as gravel and silty sand beds can also be found. These clastic sediments mainly originated from the metamorphic rocks, with a lesser amount of fragments from the limestones or the local volcanics of Bükk Mountains.

2 Methodology

2.1 Monitoring of soil movement and groundwater fluctuation

The field investigations were carried out in Avas Hill, at Miskolc city, to obtain the data required to analyze slope stability. The slope monitoring system installed on Avas Hill consists of eight small, shallow diameter observation wells to measure the changes in soil displacements (52i, 53i, 64i, and 66i) and groundwater fluctuation (51, 52i, 53i, 55, 64i, 65, 66i, 68) using inclinometer and groundwater devices, respectively (Figure 3). The groundwater level measurements were carried out weekly correlating with rainfall, and inclination measurements per month. Rainfall is one of the most common factors controlling these groundwater variations. Therefore, it was investigated for the short (per hour) and long period (per month) [43]. Based on these data and other previous data [36,37,40,44,45] that identified the lithology and general mechanical soil properties of the observation wells in the study area, we can analyze the slope stability under these conditions with other simulated parameters, for instance, the changing of the groundwater levels, construction effect (church), and soil properties.

2.2 Geological modeling

Based on the core drilling results, the geological model was constructed with two cross-sections of the fifth and sixth lines of observation wells. Golden Software Surfer 2020 was applied to illustrate the engineering geological model of the research area. Before using the program, the Global Positioning System (GPS) coordinates of the studied wells were converted from the World Geodetic

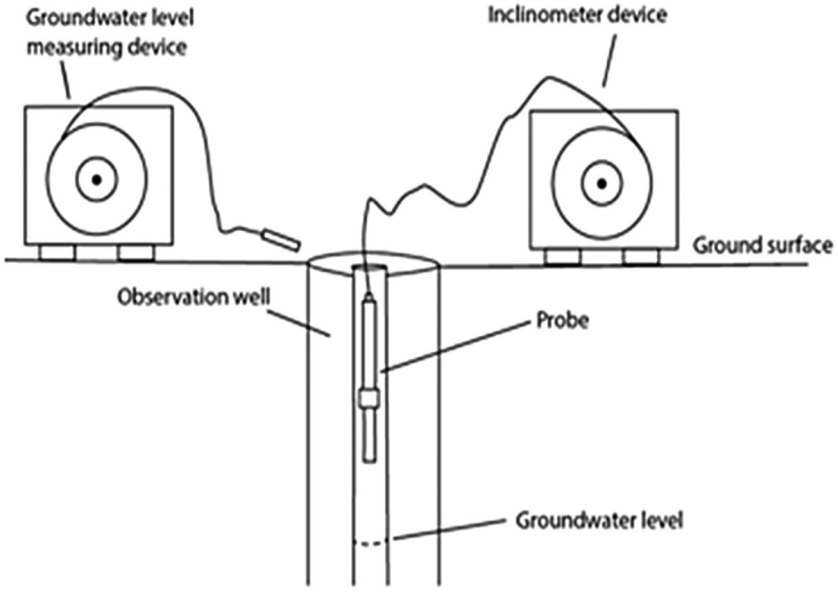

Figure 3: Schematic of the monitoring system.

Table 1: Simulated parameters input in the Surfer program for engineering geological modeling

Well no.	GPS coordinates				Elevation (m)			Groundwater level (m) (Oct., 2020)
	WGS 84		EOV					
	Latitude	Longitude	(*Y*, m)	(*X*, m)	Ground-surface	Quaternary clay	Pannonian clay	
51	48° 05′ 06.65″ N	20° 46′ 44.11″ E	778998.32	306054.61	172.822	167.489	163.389	168.392
52i	48° 05′ 05.86″ N	20° 46′ 48.18″ E	779082.82	306032.01	167.64	166.640	158.14	166.050
53i	48° 05′ 05.53″ N	20° 46′ 51.53″ E	779152.25	306023.2	160.200	159.200	150.100	155.900
55	48° 05′ 06.07″ N	20° 46′ 55.74″ E	779239.54	306042.16	150.876	149.276	140.176	145.656
64i	48° 05′ 10.72″ N	20° 46′ 34.82″ E	778803.28	306176.31	188.976	187.476	184.176	182.626
65	48° 05′ 10.68″ N	20° 46′ 43.18″ E	778975.91	306178.13	174.995	173.395	170.855	171.525
66i	48° 05′ 10.79″ N	20° 46′ 48.58″ E	779088.15	306184.84	165.202	162.602	155.702	161.942
68	48° 05′ 10.00″ N	20° 46′ 55.70″ E	779235.58	306163.64	150.876	149.276	140.176	144.996

System (WGS 84) to Unified National Projection (EOV), based on the Baltic Sea as a standard sea level for Hungary. The input data included the elevations of the ground surface, Quaternary clay, and Pannonian clay based on data obtained from the observation wells. Furthermore, the groundwater level was measured and linked with the previous elevation data (Table 1).

2.3 Evaluation of slope stability on a finite slope

The factor of safety (FS) is generally an essential parameter to evaluate slope stability. Table 2 shows the ranges of custom minimum total safety factors (F) as reported by Terzaghi and Peck [46] and recommended in the *Canadian Foundation Engineering Manual* (1992) [47]. The upper values of these total safety factors relate to normal loads and service conditions, while the lower values can be applied for maximum loads and worst geologic conditions.

Principally, the FS of the slope is the ratio between the resisting force and the driving force, and can be obtained from the following equation (1):

$$\mathrm{FS} = \frac{\text{Resisting force}}{\text{Driving force}} = \frac{\text{Shear strength}}{\text{Shear stress}}. \quad (1)$$

The shear strength of soil (τ_f) is composed of two components: cohesion and friction. It can be defined by the failure criterion of the Mohr–Coulomb [48] as illustrated in equation (2):

$$\tau_f = c + \sigma \tan \phi, \quad (2)$$

where c, σ, and ϕ denote cohesion, normal stress at rupture surface, and angle of internal friction, respectively.

Table 3 shows the limited equilibrium methods of slope stability utilized in the GEO5 program, which was

Table 2: Values of minimum overall safety factors as supposed to refs [46,47]

Failure type	Category	Safety factor range
Shearing	Earthworks	1.3-1.5
	Earth retaining structures, excavations	1.5–2
	Foundations	2–3
Seepage	Uplift, heave	1.5–2
	Exit gradient, piping	2–3

Table 3: Limited equilibrium methods of slope stability applied in the GEO5 program

Method type	Assumption	Slip surface	References
Fellenius/Petterson	Acting forces on the sides of slices are neglected	Circular	[49]
Bishop	Acting forces on the sides of slices are horizontal without acting shear force between slices		[50]
Spencer	The inter-slice forces are parallel with the same inclination. Normal forces are active on the base of the slice	Non-circular	[51]
Janbu	The inter-slice normal force location is defined by the thrust line		[52]
Morgenstern-price	The inter-slice shear and inter-slice normal forces are related to each other. Normal forces act on the base of the slice		[53]

applied to calculate the values of FS based on different analytical methods such as Fellenius/Petterson [49], Bishop [50], Spencer [51], Janbu [52], and Moregenstern-price [53]. These methods were classified based on the shape of the slip surface, which is known as a failure surface or surface of sliding where the soils or rocks slip. The slip surface has four types: circular, non-circular, transitional, and compound [54,55]. FS calculations were conducted based on the Bishop Optimization method under the following conditions: before and after the construction of the church and retaining system, as well as groundwater dropping.

This program is a finite element program that was designed to find solutions to geotechnical problems. The main advantages of the GEO5 program are analysis of the slope situation, finding the problems, accuracy improving, and saving time. Besides, it can be used after a long time of work break to modify the structure design. GEO5 program has used standard information and knowledge in many countries based on common and well-known theories. The program has complaints with Eurocode 7 (EN 1997-1) [56] and LRFD (AASHTO standards) [57].

Generally, the Bishop method is the most widely used technique nowadays [58]. It is used to identify the highest optimum critical slip surface of the slope. When it is used in the GEO5 program, accurate and satisfactory results can be obtained. Here, the settings of the program were adjusted based on the cross-sections of the fifth and sixth line observation wells. These cross-sections were obtained from the Golden Software Surfer 2020. Also, the standard of FS was set at about 1.5 in this study.

2.3.1 Evaluation of groundwater fluctuation and construction influences

The simulated parameters of layers (Table 4) associated with those of the groundwater levels and dimensions of the church (Tables 5 and 6) were used as input data in the GEO5 program to calculate the FS before and after the groundwater level fluctuations and construction effects of the church on the finite slopes, respectively. These parameters were obtained based on the standard values of soil types involved in the GEO5 program. These parameters, such as unit weight (γ), internal friction angle (ϕ_{ef}), soil cohesion (c_{ef}), and saturated unit weight (γ_{sat}), are listed in Table 2. The church built on the eastern slope of the Avas Hill between the lines of the fifth and sixth observation wells affected slope stability (Figure 1). The

Table 4: Simulated strength parameters of the layers input in the GEO5 program to calculate the FS before and after the groundwater fluctuations and construction

Parameters	Landfill	Quaternary clay	Pannonian clay
γ (kN/m^3)	20.00	20.50	18.50
ϕ_{ef} (°)	36.50	15.00	24.50
c_{ef} (kPa)	0.00	5.00	14.00
γ_{sat} (kN/m^3)	20.00	20.50	18.50

Table 5: Groundwater level coordinate data input in the GEO5 program

Well no.	Line No.			
	Fifth		Sixth	
	(*X**, m)	(*Z***, m)	(*X**, m)	(*Z***, m)
51	0.00	1.48	—	—
52iu	2.87	1.01	—	—
53iu	4.66	0.64	—	—
55	6.10	0.25	—	—
64i	—	—	0.00	1.30
65	—	—	2.43	0.92
66i	—	—	3.93	0.65
68i	—	—	6.10	0.29

*Represents the horizontal coordinate (distance) of a finite slope in the GEO5 program.
**Represents the vertical coordinate (elevation) of a finite slope in the GEO5 program.

Table 6: Simulated parameters of surcharge (church) input in the GEO5 program

Length (m)	Width (m)	Height (m)	Magnitude (kN/m^2)	Slope (°)
78.37	34.84	13–16	500	8

Table 7: Simulated strength parameters of frontfill, backfill, and soil foundation input in the GEO5 program for setting up the retaining system

γ (kN/m^3)	ϕ_{ef} (°)	c_{ef} (kPa)	γ_{sat} (kN/m^3)
19	32.5	4	19

groundwater levels and construction effect data were obtained based on the cross-sections of the fifth and sixth line observation wells. These cross-sections were obtained from the Surfer program.

Table 8: Simulated parameters of the gravity retaining wall system input in the GEO5 program

Parameters			Line fifth	Line sixth
Material of wall structure	Concrete	f_{ck} (MPa)	80	80
		f_{ctm} (MPa)	4.8	4.8
	Reinforcing steel bars	f_{yk} (MPa)	500	500
	γ (kN/m^3)		23	23
Foundation soil	Geometry	Thickness (m)	0.7	1
		Offset left (m)	0.5	0.7
		Offset right (m)	0.5	0.7
	Soil type		Silty gravel	Silty gravel
Frontfill	Thickness (m)		1	1
	Soil type		Silty gravel	Silty gravel
Backfill	Slope (°)		45	45
	Soil type		Silty gravel	Silty gravel
Groundwater level	In front of construction (m)		4.5	4.5
	Behind construction (m)		1.5	4.5

2.3.2 Influence of the retaining system

Retaining systems include many types of retaining structures such as gravity walls, cantilever retaining walls, fort-counter retaining walls, anchors retaining walls, or piled retaining walls [58–60]. In this study, the gravity retaining wall was constructed to increase the shear strength of soil in the fifth and sixth lines of observation wells. This type is the most commonly applied due to its economical features, so it was selectively nominated. Concrete and gravel are the two components of this gravity retaining wall. Concrete is one of the most common and effective materials used to construct a shield against artificial or natural hazards [61–65].

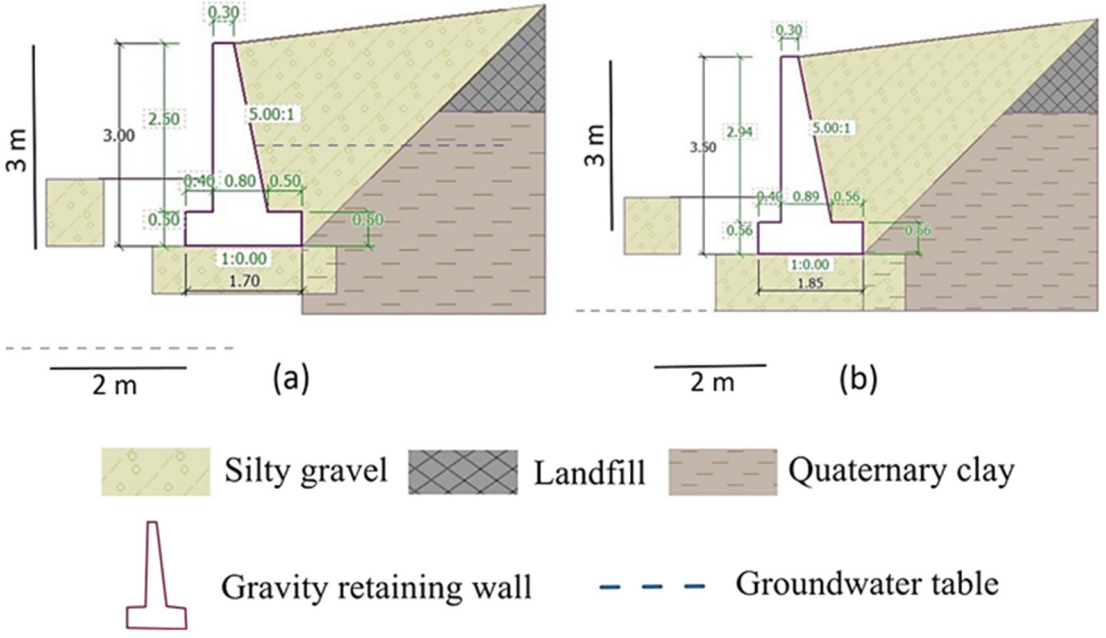

Figure 4: Simulated dimensions of gravity retaining walls in the slope of: (a) fifth observation wells and (b) sixth observation wells.

The simulated parameters of the gravity retaining system input in the GEO5 program are related to the fifth and sixth line observation wells. The used parameters are listed in Tables 7 and 8. These parameters include foundation soil, frontfill, and backfill, which are composed of silty gravel (Table 7). Table 8 shows the groundwater level and parameters of the material used in the wall structure such as compressive strength (f_{ck}) and tensile strength (f_{ctm}) of concrete, yield strength (f_{yk}) of the reinforcing steel bars, and unit weight of the wall (γ). Figure 4 illustrates the simulated dimensions of the gravity retaining system based on the fifth and sixth lines.

3 Results and discussion

3.1 Monitoring

3.1.1 Soil movement

As shown in Figure 5, the results of the inclinometer measurements show that there is a type of soil movement with a displacement of nearly 2 mm/year in an oblique direction toward the NW–NE from April 2018 to November 2020. Compared to the measurements conducted in April 2018, the recent measurements (Figure 5) show that the soil movement was more effective on the uppermost first 5 m of the soil. In the first 3 m of the uppermost soil, the displacement rate is about 2 mm/year toward the NW direction of the two first meters and NE direction to the rest. After that, this rate decreases to zero value at about 5 m. After 5 m, the displacement becomes not active.

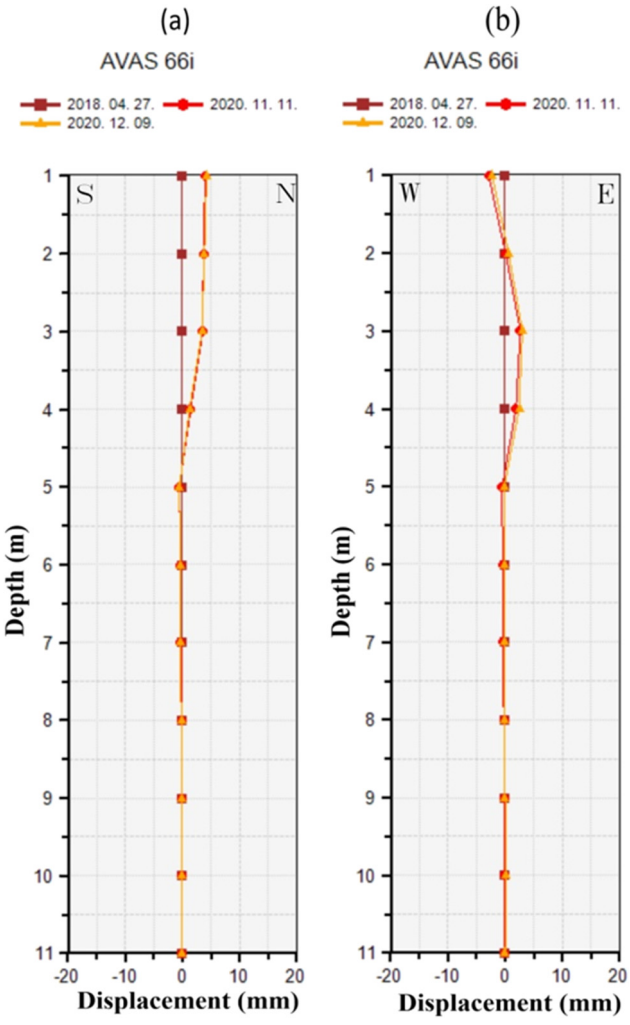

Figure 5: Cross-section views show the relationship between the rates of soil displacements and depth at the observation wells of 66i from: (a) N–S direction and (b) E–W direction.

3.1.2 Groundwater fluctuation

Groundwater fluctuation is one of the main reasons for slope instability [66,67]. The hydrogeological map of the study area illustrates that groundwater is accumulated in the east–southeast of Avas based on data collected from the observation wells (Figures 6 and 7). The pore pressure of water reduces the soil effective stresses and consequently the soil shear strength [68]. Subsequently, a severe hazard leads to the collapse of the ground surface and the construction.

Compared to the rainfall level, the monitoring data of underground water level does not indicate a connected aquifer. This is illustrated in Figure 7, where the levels of rainfall and underground water are not consonant. This can be attributed to both natural and artificial factors. The natural one is related to the lithological composition of the underlying impermeable soil, which is composed of clay and sandy clay (Figure 8), while the artificial ones (Figure 8) include leakage from the network pipeline, construction pits, or construction of the deep foundation [35]. Additionally, the impermeable coverage of the asphaltic layer capping the road of the area plays an influential role in the changes in underground water levels. This can be assigned to its predominance of joints and tensional cracks (Figure 9), which contribute to the infiltration of surface water (i.e., rainfall, runoff, the water of freeze-thaw, etc.) into the ground [33]. These cracks can be attributed to the weak strength of the upper landfill layer [38].

Although the infiltration is responsible for slope failure [16,69], this is not achieved in this study. This can be

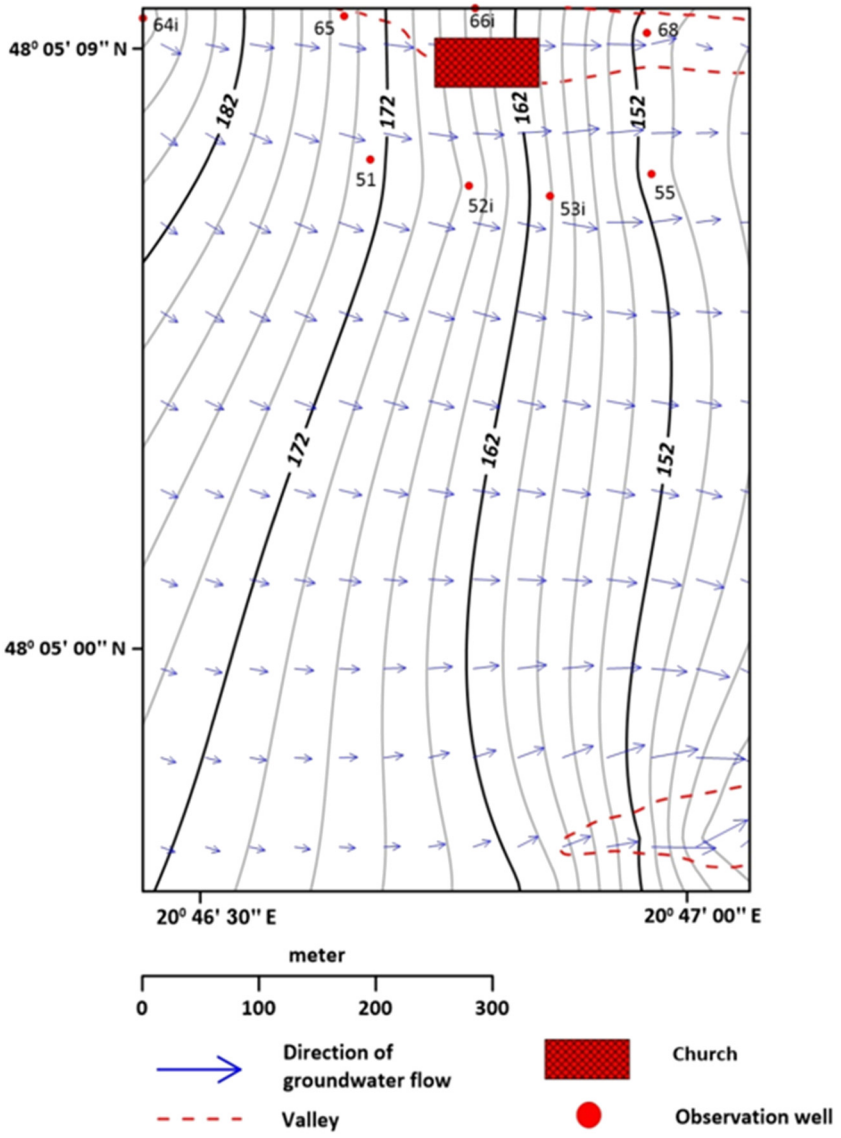

Figure 6: Groundwater flows from the West part of the study area into the East–Southeast.

attributed to the artificial drainage systems (e.g., drainage ditches), which were constructed to reduce the infiltration of slope water into the ground (Figure 10).

3.2 Engineering geological modeling

Figure 11 illustrates the engineering geological modeling of the eastern side of Avas Hill, which was drawn with the knowledge of the two lines of observation wells (fifth and sixth) having 4.5–10 m depth. This modeling shows that the Avas Hill consists of two layers, Quaternary (mainly reddish-brown to brown clay) and Pannonia (dominantly brownish clay and sandy clay), according to GeoExpert Geotechnikai tervező és szakértő Kft, 2013. Also, it is deduced that the slope dips to the east, and the two geological profiles of the two lines of observation wells (fifth and sixth).

The modeling shows (Figure 11a) that the church is constructed in an erosive valley where erosion and weathering of soil take place. Subsequently, it is a disadvantage of engineering geology when the constructed buildings were established on the valley floor instead of the flat area. The thickness of the Quaternary clay layer varies in the two geological cross-sections ranging from 16.67–18.33 to 9.21–23.68 m toward the eastern direction of the fifth and sixth slopes, respectively (Figure 11b and c).

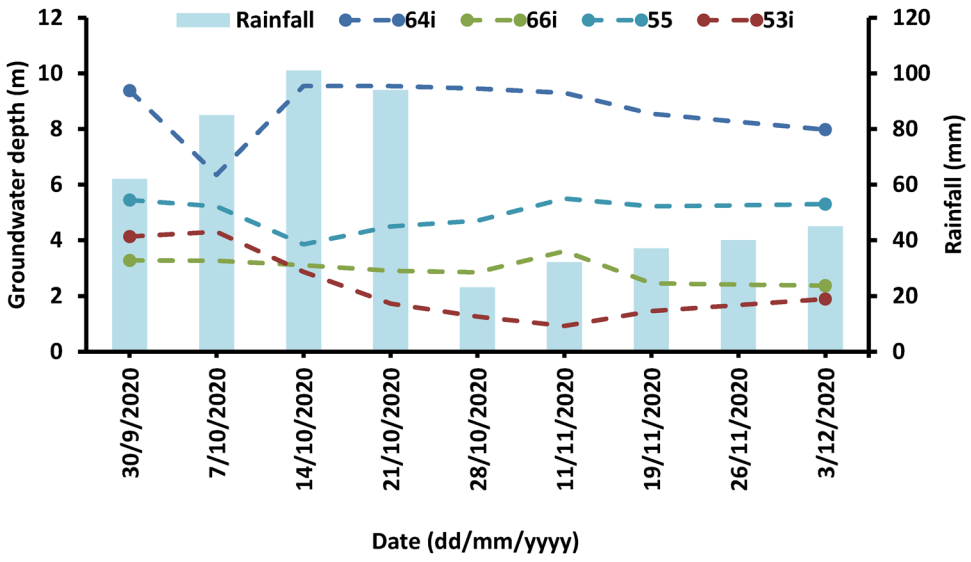

Figure 7: Relationship between Groundwater and rainfall levels for about 2.5 months.

The difference in the thickening of this layer between the two slopes (fifth and sixth) could reflect the variation in the topographic surface. The accumulated soil deposits on the downslope occurring as a result of soil movements can lead to the thickening of the Quaternary clay layer. In contrast, the erosion and weathering processes can lead to the thinning of this layer.

3.3 Evaluation of slope stability on a finite slope

3.3.1 Slope stability modeling

Based on the simulated results observed in Figure 12, the FS of the two slopes ranges between 1.29 and 1.47, and

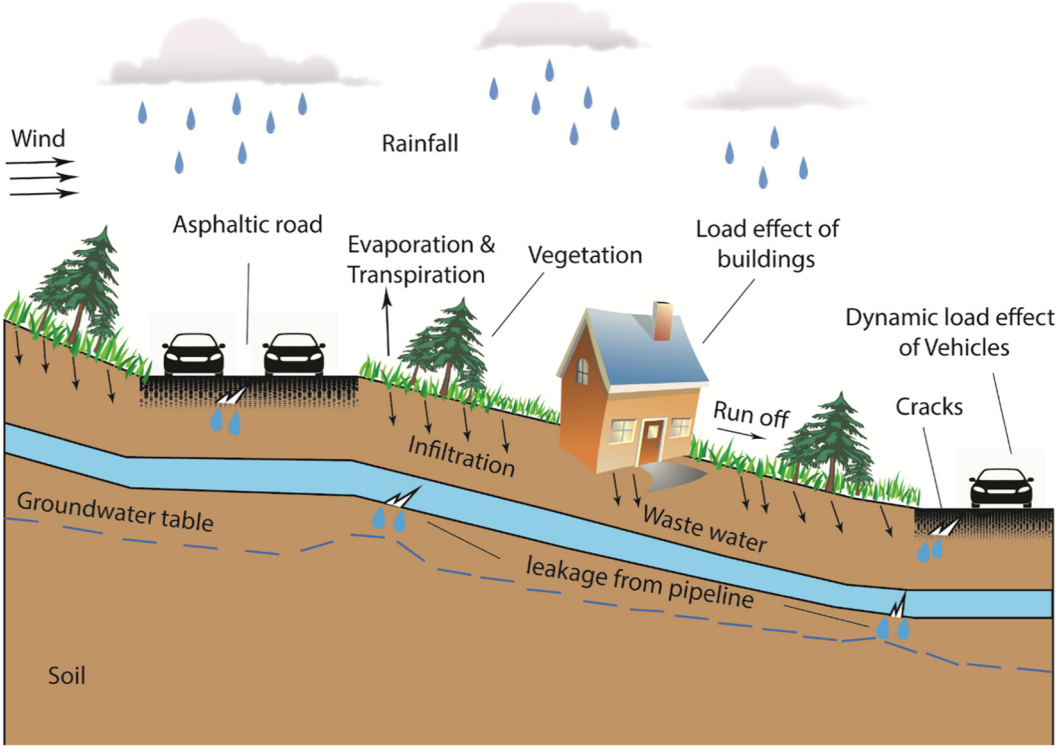

Figure 8: Detailed schematic illustrates several factors affecting groundwater levels.

Figure 9: Tensional cracks in the asphalt coverage of the study area.

this range is less than 1.5 (the critical value of stable slope). So, these values indicate that the current states of the two slopes are unstable [70]. Moreover, the critical slip surface is observed within a shallow depth below the Quaternary clay deposits in the fifth and sixth lines of observation wells based on the Bishop Optimization method using the GEO5 program (Figure 13). It indicates that the layers of Quaternary clay and landfill and their overlaying building (church) are threatened by the sliding on the Pannonian surface.

3.4 Influence of groundwater fluctuation on slope stability

Based on the simulated results obtained from the GEO5 program (Figure 14), the groundwater level falls 40 cm in depth as shown in Figure 15. After that, the ranges of FS at the two lines of fifth and sixth observation wells increase from 1.29–1.47 to 1.33–1.51 (Figure 14). Consequently, the slope stability increases due to the reduction in the pore-water pressure and the rise in soil friction. Additionally, the uplift pressure induced by the confined water decreases under the sliding surface. Moreover, the lithology of the soil (Quaternary–Pannonian sequence) is composed of highly plastic clay minerals (i.e., montmorillonite). As commonly known, montmorillonite has a destructive drawback on slope stability due to its low shearing strength and high swelling ability [71,72]. Furthermore, groundwater fluctuation has a significant effect on the radius of the critical slip surfaces [73]. This can be observed from the radius critical slip surface at the fifth line observation wells when it decreases and moves

Figure 10: Drainage ditch (artificial systems) to diminish slope water infiltration.

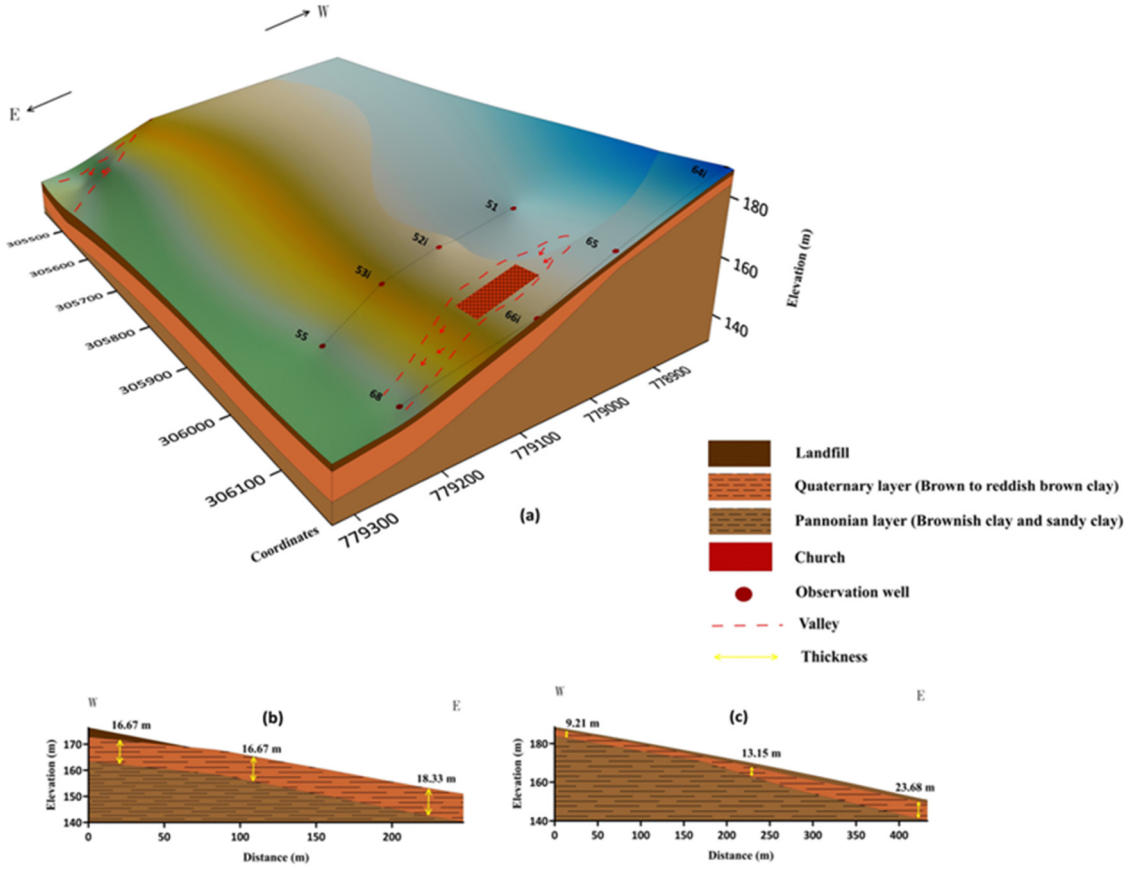

Figure 11: (a) Engineering geological modeling of the eastern side of Avas Hill. The red dashed lines indicate the erosive valleys, (b) a profile illustrates the cross-section of fifth line observation wells, and (c) a profile illustrates the cross-section of sixth line observation wells.

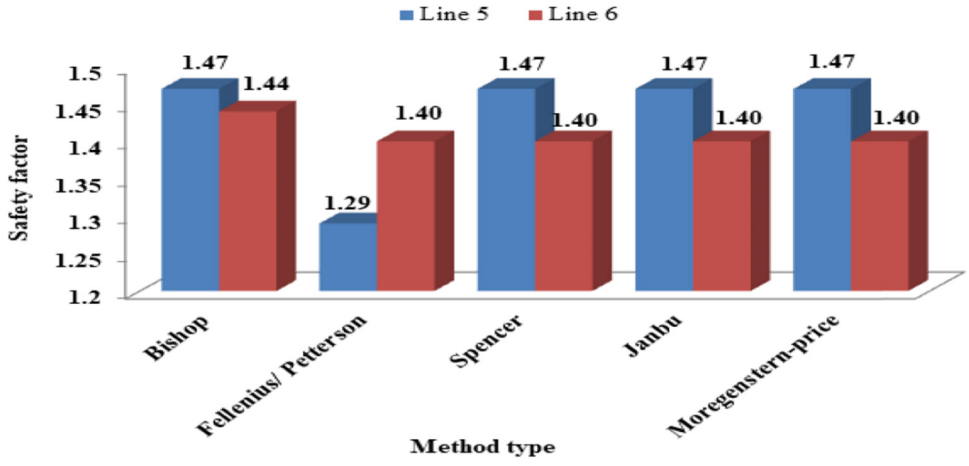

Figure 12: FS of the observation wells on the fifth and sixth lines based on the limited equilibrium methods of slope stability.

from being tangential to the Quaternary–Pannonian interface to be within the Quaternary clay layer (Figure 15). This occurs when the groundwater level drops. Therefore, the volume of soil movements decreases on the slope (Figure 15).

3.4.1 Influence of construction on slope

After applying different analytical methods (Figure 16), the results obtained from the fifth and sixth lines show that the slope became unstable after constructing the church,

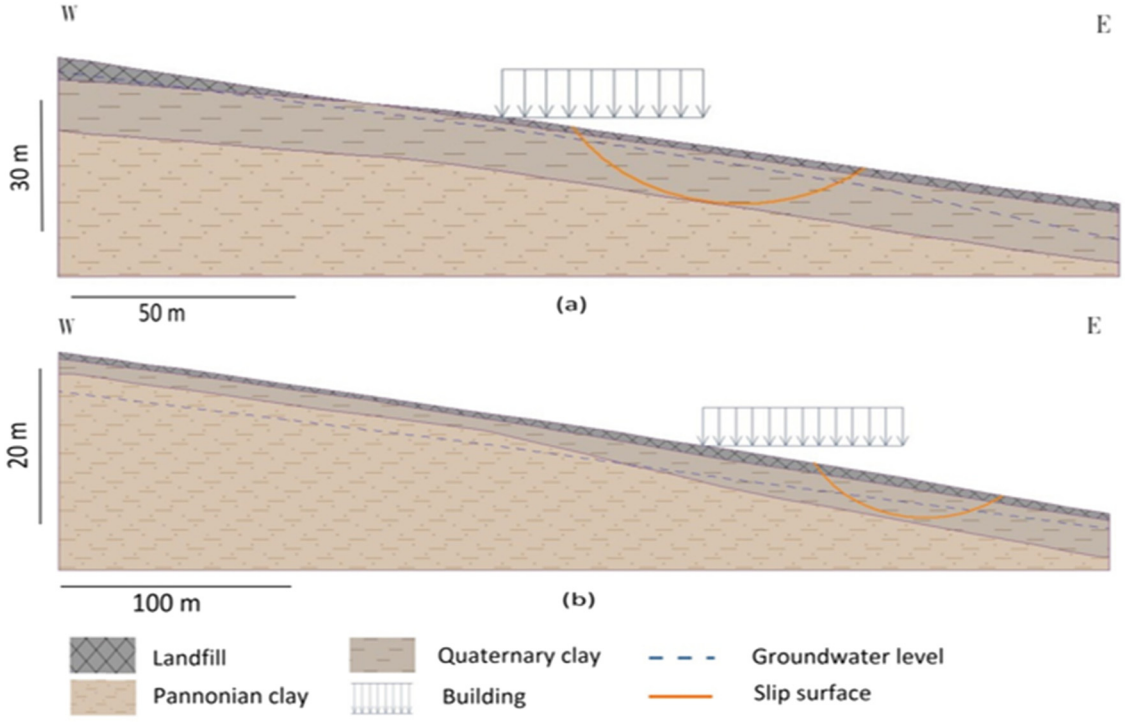

Figure 13: Analysis models illustrate the slope stability of (a) fifth observation wells and (b) sixth observation wells.

and that the the FS of the slope is less than 1.5. However, before constructing the church, the FS was higher than the value of the critical standard. Therefore, the church decreased the shear strength of the soil resulting in a negative impact on slope stability. Figure 17 illustrates that the critical slip surface was located near the ground surface at the landfill layer before constructing the church. However, it shifted deeper into the underground reaching the Quaternary–Pannonian boundary of the sixth line observation wells after construction of the church. As a result, the volume of soil movements increased after construction of the church compared to what it was before.

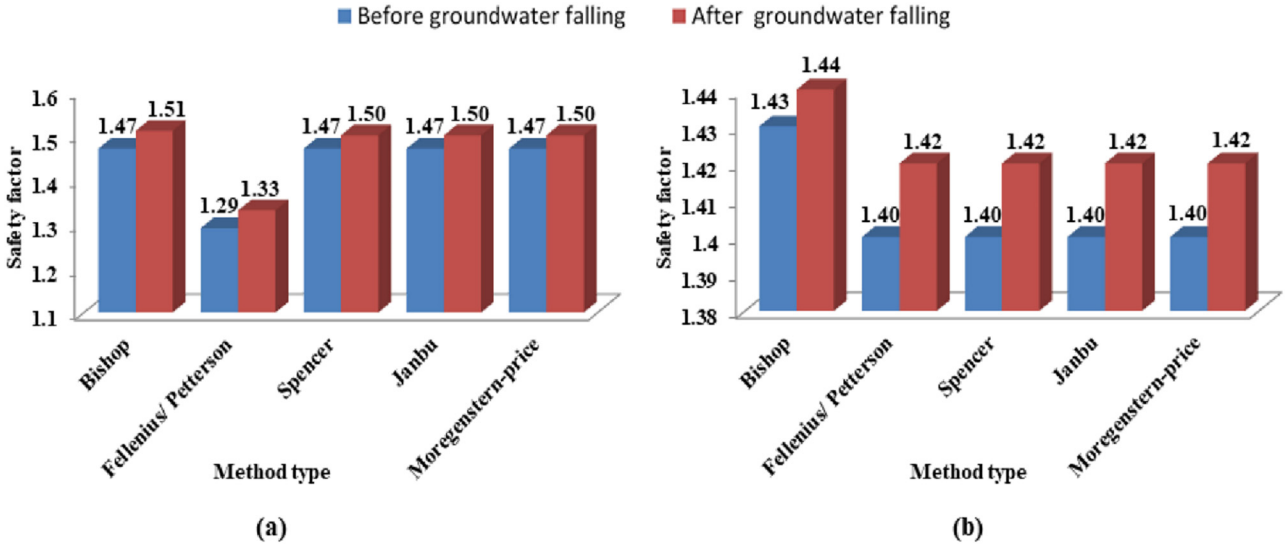

Figure 14: The influence of groundwater fluctuation on slope stability based on limited equilibrium methods at (a) the fifth line observation wells and (b) the sixth line observation wells.

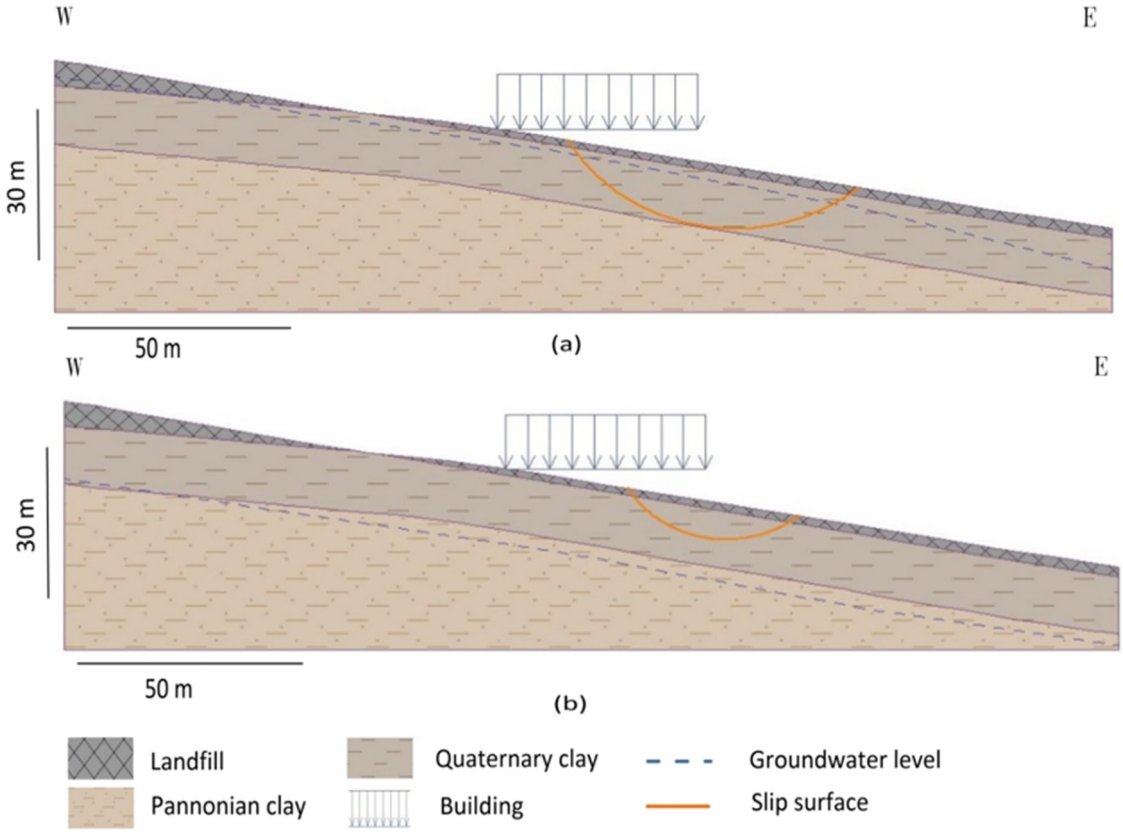

Figure 15: Analysis models illustrate the slope stability of the fifth line observation wells after the fall in the groundwater level from (a) to (b) by about 40 cm.

3.4.2 Influence of different retaining structures

The simulated results (Figure 18) show that the construction of a gravity retaining wall system has enhanced slope stability. This can be observed by the increasing FS at the fifth and sixth lines of observation wells from 1.29–1.47 to 1.56–1.84 after the construction of the retaining systems (Figure 18). Figure 19 illustrates that the analysis

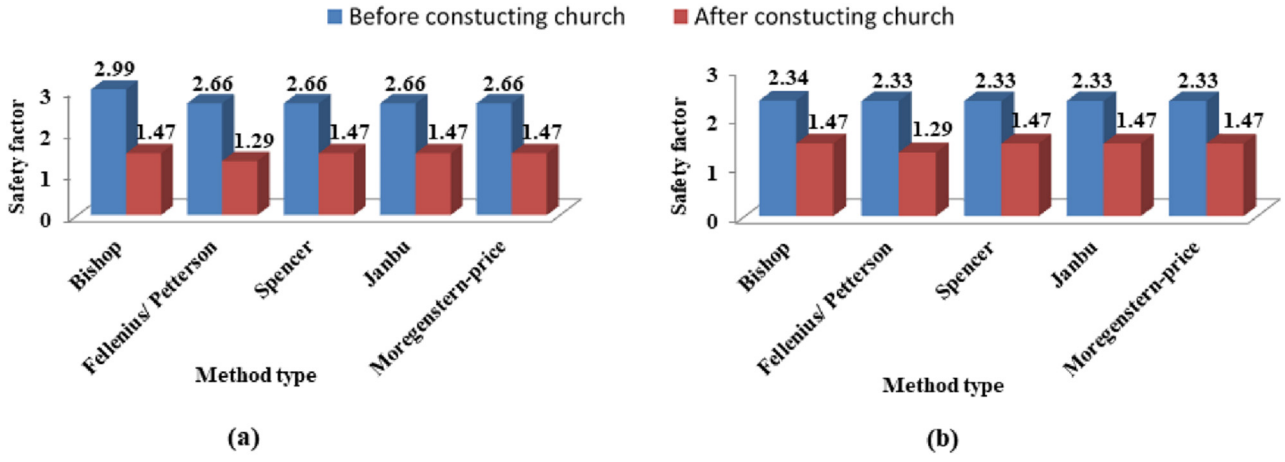

Figure 16: The influence of the construction on slope stability based on the limited equilibrium method at (a) the fifth line observation wells and (b) the sixth line observation wells.

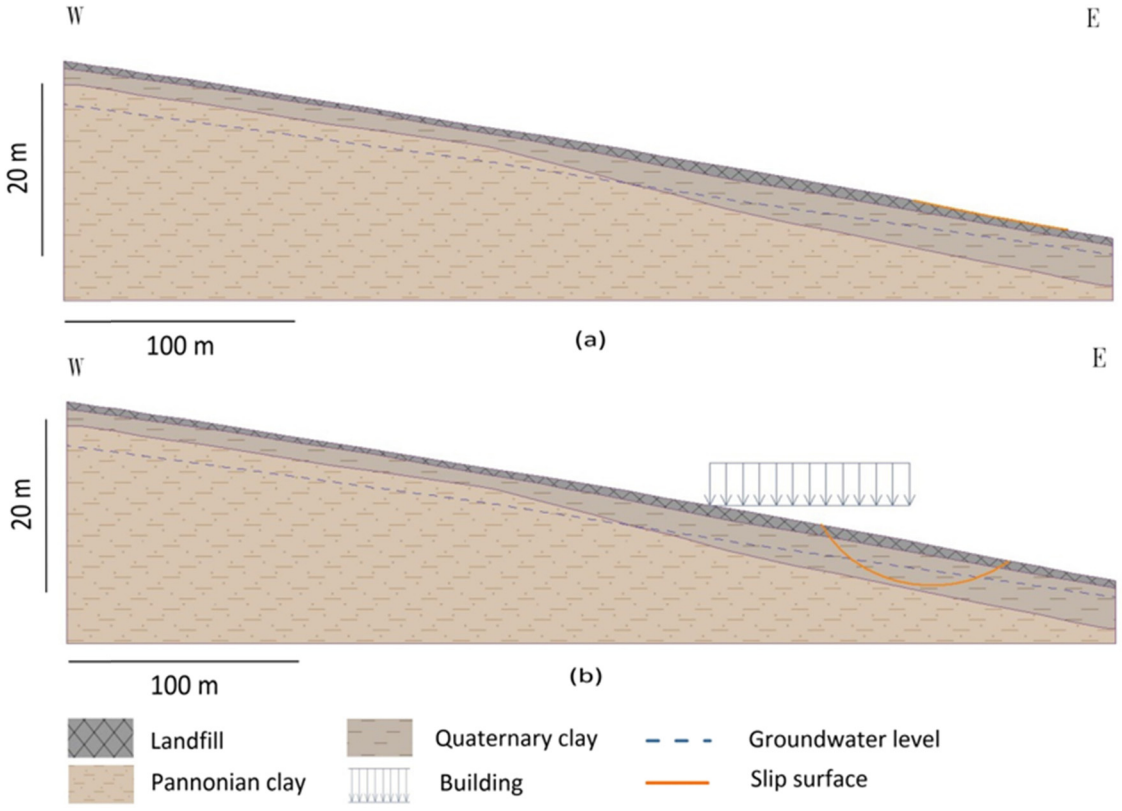

Figure 17: Analysis models illustrate the slope stability of the sixth line observation wells: (a) before constructing the church and (b) after constructing the church.

models of the fifth and sixth lines of observation wells have the same FS value, which is equal to 1.83 based on the Bishop Optimization method [50]. Moreover, the position of the critical slip surface has shifted from the lower to the upper part of the Quaternary clay layer reflecting the reduction in the volume of soil movements.

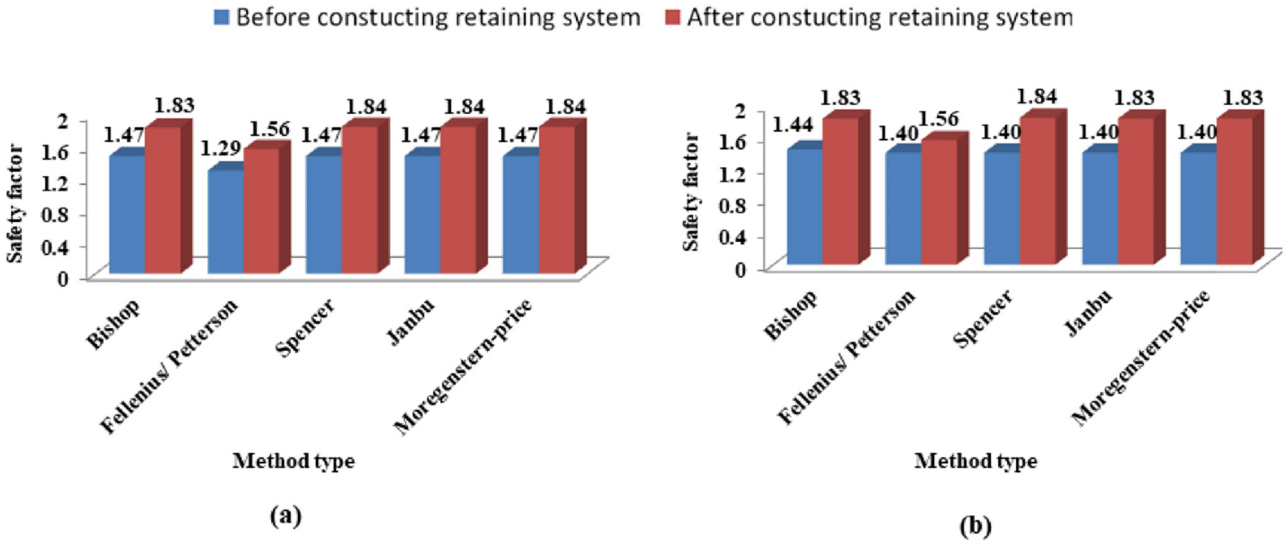

Figure 18: The influence of the gravity retaining wall system based on the limited equilibrium methods of slope stability on (a) the fifth line observation wells and (b) the sixth line observation wells.

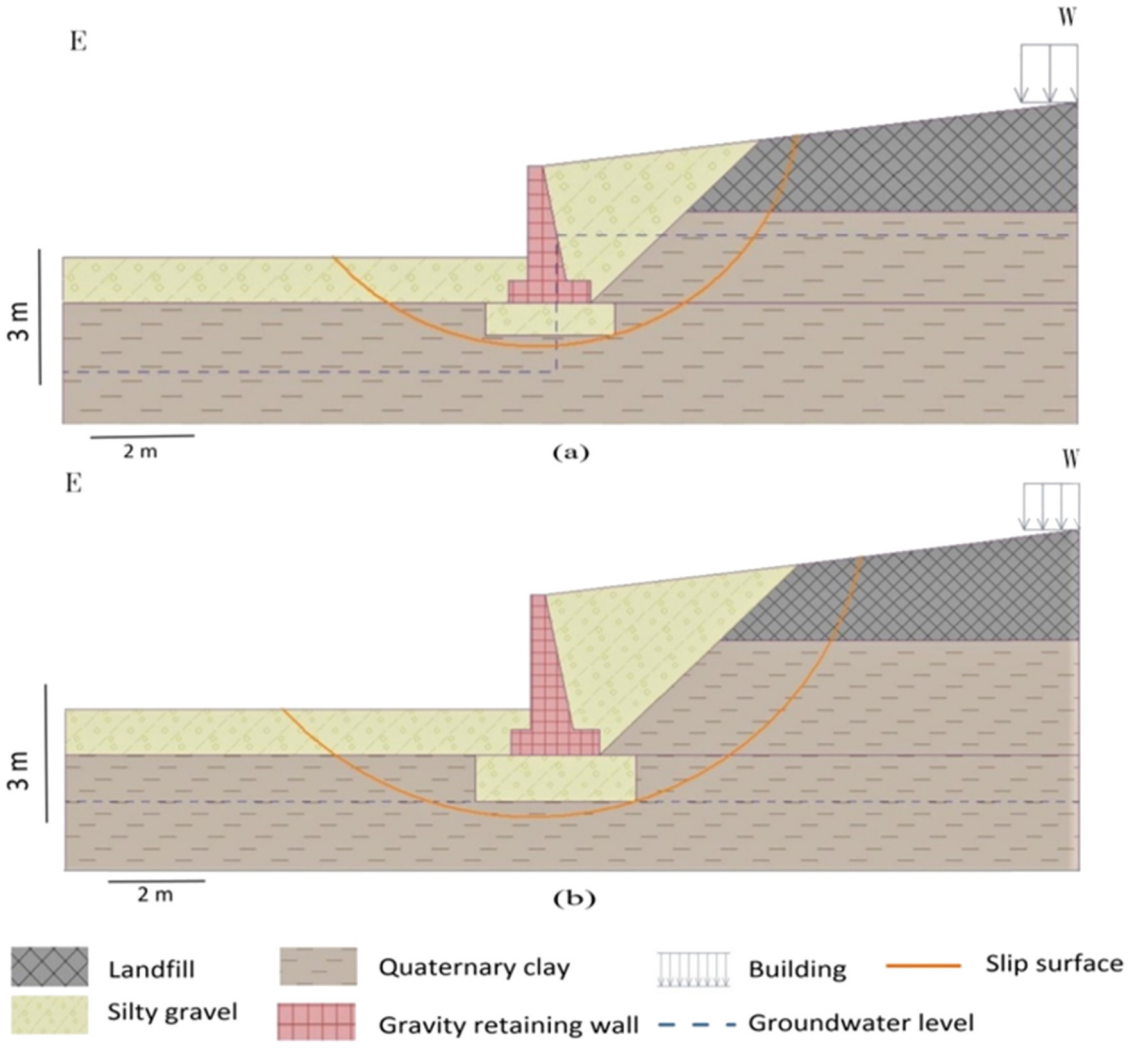

Figure 19: Analysis models illustrate the slope stability after constructing the gravity retaining system of (a) the fifth line observation wells and (b) the sixth line observation wells.

4 Conclusion

Based on the experimental and simulated results, the following deductions can be drawn:

1. The soil movement is more influential on the first 5 m of the soil: the displacement rate is equal to 2 mm/year toward the NW–NE direction. After 5 m, the soil movements are inactive.
2. There is no relationship between rainfall and underground water level fluctuation due to the following reasons:
   a) Natural aspects related to the underlying soil composed of impermeable clay and sandy clay.
   b) Artificial aspects included leakage from the network pipeline, drainage network, construction pits, or construction of the deep foundation. Otherwise, the cracked asphaltic layer covering the roads contributes to surface water percolation (i.e., runoff, rainfall, the water of freeze-thaw, etc.) into the ground.
3. The safety factor of the study area is less than 1.5 indicating that the slope is rather unstable. Besides, the critical slip surfaces are optimized below the Quaternary clay layer. This will create a hazard for the church built above these deposits.
4. The fluctuations in groundwater levels have both deleterious and beneficial impacts on slope stability in the study area. The deleterious one is due to groundwater levels rising owing to the pore-water pressure released in the soil and the swelling property of the montmorillonite composing the soil. The beneficial one is the decrease in soil movements due to falling groundwater levels.
5. The recently built structures have a pernicious effect on slope stability when it is constructed on the middle

slope. These structures are susceptible to soil movements at any time. So, it is not recommended to build any structures on the slope except at the summit of the slope (i.e., the plateau area).

6. Based on the simulated results of slope models, the recently built structures can be supported against the soil movements on the slope by constructing retaining wall systems such as gravity retaining walls.

Acknowledgment: The authors are very grateful to Prof. György Less, Institute of Mineralogy and Geology, University of Miskolc, Hungary, for help in the field as well as Miss Udomp P. Udomp, Mr Arbi Ben Aoun and Mr Alaa E. Abbadi, Institute of Environmental Management, University of Miskolc, Hungary, for help in the software analysis. The authors are also grateful to the Embassy of the Arab Republic of Egypt and Egypt's Office for Cultural and Educational Relations, Vienna.

Author contributions: E.H. and T.K. designed and led the study. E.H. and M.A.M. wrote the manuscript of this work. T.K., E.H., A.T., and M.A.M. analyzed the data of the article. A.T. helped and contributed to the fieldwork. All authors contributed to the writing and gave final approval of this paper

Conflict of interest: The author has not declared any conflicts of interest.

References

[1] Kjekstad O, Highland L. Economic and social impacts of landslides. Landslides–disaster risk reduction. Berlin: Springer; 2009. p. 573–87.
[2] Chae B-G, Park H-J, Catani F, Simoni A, Berti M. Landslide prediction, monitoring and early warning: a concise review of state-of-the-art. Geosci J. 2017;21:1033–70.
[3] Hansen M. Strategies for classification of landslides. Slope instability. New York: Wiley & Sons; 1984. p. 1–25.
[4] Yin K, Chen L, Zhang G. Regional landslide hazard warning and risk assessment. Earth Sci Front. 2007;14:85–93.
[5] Brönnimann CS. Effect of groundwater on landslide triggering: école polytechnique Fédérale de Lausanne. Switzerland: EPFL; 2011.
[6] Mori A, Subramanian SS, Ishikawa T, Komatsu M. A case study of a cut slope failure influenced by snowmelt and rainfall. Proc Eng. 2017;189:533–8.
[7] Hong Y, Hiura H, Shino K, Sassa K, Suemine A, Fukuoka H, et al. The influence of intense rainfall on the activity of large-scale crystalline schist landslides in Shikoku Island, Japan. Landslides. 2005;2:97–105.
[8] Zhao Y, Li Y, Zhang L, Wang Q. Groundwater level prediction of landslide based on classification and regression tree. Geod Geodyn. 2016;7:348–55.
[9] Xiong X, Shi Z, Xiong Y, Peng M, Ma X, Zhang F. Unsaturated slope stability around the Three Gorges Reservoir under various combinations of rainfall and water level fluctuation. Eng Geol. 2019;261:105231.
[10] Wei Z-l, Lü Q, Sun H-Y, Shang Y-Q. Estimating the rainfall threshold of a deep-seated landslide by integrating models for predicting the groundwater level and stability analysis of the slope. Eng Geol. 2019;253:14–26.
[11] Troncone A, Pugliese L, Conte E. Run-out simulation of a landslide triggered by an increase in the groundwater level using the material point method. Water. 2020;12:2817.
[12] Jones S, Kasthurba AK, Bhagyanathan A, Binoy BV. Impact of anthropogenic activities on landslide occurrences in south-west India: an investigation using spatial models. J Earth Syst Sci. 2021;130:70.
[13] Pande A, Joshi RC, Jalal DS. Selected landslide types in the Central Himalaya: their relation to geological structure and anthropogenic activities. Environmentalist. 2002;22:269–87.
[14] Kokutse NK, Temgoua AGT, Kavazović Z. Slope stability and vegetation: Conceptual and numerical investigation of mechanical effects. Ecol Eng. 2016;86:146–53.
[15] Emadi-Tafti M, Ataie-Ashtiani B, Hosseini SM. Integrated impacts of vegetation and soil type on slope stability: A case study of Kheyrud Forest, Iran. Ecol Model. 2021;446:109498.
[16] Eab KH, Likitlersuang S, Takahashi A. Laboratory and modeling investigation of root-reinforced system for slope stabilisation. Soils Found. 2015;55:1270–81.
[17] Nguyen TS, Likitlersuang S, Jotisankasa A. Stability analysis of vegetated residual soil slope in Thailand under rainfall conditions. Env Geotech. 2020;7:338–49.
[18] Likitlersuang S, Takahashi A, Eab KH. Modeling of root-reinforced soil slope under rainfall condition. Eng J. 2017;21:123–32.
[19] Fondjo AA, Theron E, Ray RP. Stabilization of expansive soils using mechanical and chemical methods: a comprehensive review. Civ Eng Archit. 2021;9:1295–308.
[20] Zu R, Khalid U, Farooq K, Mujtaba H. On yield stress of compacted clays. Int J Geotech Eng. 2018;9:21.
[21] Bakhshi Ardakani S, Rajabi AM. Laboratory investigation of clayey soils improvement using sepiolite as an additive; engineering performances and micro-scale analysis. Eng Geol. 2021;293:106328.
[22] Rajabi AM, Ardakani SB. Effects of natural-zeolite additive on mechanical and physicochemical properties of clayey soils. J Mater Civ Eng. 2020;32:04020306.
[23] Khodaparast M, Rajabi AM, Mohammadi M. Mechanical properties of silty clay soil treated with a mixture of lime and zinc oxide nanoparticles. Constr Build Mater. 2021;281:122548.
[24] Ngo TP, Likitlersuang S, Takahashi A. Performance of a geosynthetic cementitious composite mat for stabilising sandy slopes. Geosynth Int. 2019;26:309–19.
[25] Nguyen TS, Likitlersuang S, Jotisankasa A. Influence of the spatial variability of the root cohesion on a slope-scale stability model: a case study of residual soil slope in Thailand. Bull Eng Geol Env. 2019;78:3337–51.

[26] Leknoi U, Likitlersuang S. Good practice and lesson learned in promoting vetiver as solution for slope stabilisation and erosion control in Thailand. Land Use Policy. 2020;99:105008.
[27] Likitlersuang S, Kounyou K, Prasetyaningtiyas GA. Performance of geosynthetic cementitious composite mat and vetiver on soil erosion control. J Mt Sci. 2020;17:1410–22.
[28] Chen G, Jia J. Case study of slope stabilization using compression anchor and reinforced concrete beam. Boundaries of Rock Mechanics. London: CRC Press; 2008. p. 475–8.
[29] Jamsawang P, Voottipruex P, Jongpradist P, Likitlersuang S. Field and three-dimensional finite element investigations of the failure cause and rehabilitation of a composite soil-cement retaining wall. Eng Fail Anal. 2021;127:105532.
[30] Troncone A, Pugliese L, Lamanna G, Conte E. Prediction of rainfall-induced landslide movements in the presence of stabilizing piles. Eng Geol. 2021;288:106143.
[31] Wei Z-L, Wang D-F, Xu H-D, Sun H-Y. Clarifying the effectiveness of drainage tunnels in landslide controls based on high-frequency in-site monitoring. Bull Eng Geol Env. 2020;79:3289–305.
[32] Ukritchon B, Chea S, Keawsawasvong S. Optimal design of Reinforced Concrete Cantilever Retaining Walls considering the requirement of slope stability. KSCE J Civ Eng. 2017;21:2673–82.
[33] Kotiukov P, Lange IY. Engineering Geological Analysis of the Landslide Causes During the Construction of Industrial Building. Int J Civ Eng Technol. 2019;10:1471–8.
[34] Szabó J. The relationship between landslide activity and weather: examples from Hungary. Nat Hazards Earth Syst Sci. 2003;3:43–52.
[35] Mocsár-Vámos M, Görög P, Török Á. Engineering geological characterization of the host rocks of underground cellars in Avas hill, Northern Hungary. Geotech Eng Infrastruct Dev. 2015;2287–92.
[36] Ringer Á, Miskolci Avas A. A felszínfejlődés fő kérdései (The Avas Hill in Mis-kolc. Basic Questions of the landscape evolution). In Miskolci Avas A, editor. A Miskolci Her-man Ottó Múzeum és a Borsodi Ny közös kiadványa Miskolc. 1933;49–53.
[37] Schréter Z. A miskolci Avas pincebeomlásai (Collapses of vine cellars on the Avas Hill, Miskolc). MÁFI Évi Jel. 1940;35:1741–54.
[38] Mocsár-Vámos M, Görög P, Borostyáni M, Vásárhelyi B, Török Á. Stability analysis of wine cellars cut into volcanic tuffs in Northern Hungary. In: Lollino G, Giordan D, Marunteanu C, Christaras B, Yoshinori I, Margottini C, editors. Engineering geology for society and territory. Vol. 8. Cham: Springer International Publishing; 2015. p. 153–7.
[39] Vámos M, Görög P, Vásárhelyi B. Landside problem and its investigations in Miskolc (Hungary). In: Lollino G, Manconi A, Guzzetti F, Culshaw M, Bobrowsky P, Luino F, editors. Engineering geology for society and territory. Vol. 5, Cham: Springer International Publishing; 2015. p. 873–7.
[40] Papp K. Miskolcz környékének geológiai viszonyai (Geology of Miskolc). A Magy Királyi Földtani Intézet Évkönyve. 1907;16:91–132.
[41] Hajdúné K. Az Avas geológiai felépítése (Geology of the Avas). In: Miskolci Avas A, Herman A, editors. Ottó Múzeum és a Borsodi Nyomda közös kiadványaOttó Múzeum és a Borsodi Nyomda közös kiadványa. Miskolc; 1993. p. 49–53.
[42] Hartai E, Szakáll S. Geological and mineralogical background of the Palaeolithic chert mining on the Avas Hill, Miskolc, Hungary. Praehistoria. 2005;6:15–21.
[43] Nguyen TS, Likitlersuang S, Ohtsu H, Kitaoka T. Influence of the spatial variability of shear strength parameters on rainfall induced landslides: a case study of sandstone slope in Japan. Arab J Geosci. 2017;10:369.
[44] Fekete Z, Kántor T, Tóth M. Slope observation network of eastern Avas in Mis-kolc. XV-KMKTK-Poszter: Institute of Environmental Management, University of Miskolc, Hungary IH-3515 Miskolc-Egyetemváros; 2019.
[45] Mohamed E, Tamas K. Geotechnical investigations: a case study of Avas hill, Miskolc, Northeast of Hungary. A Miskolci Egyetem, Műszaki Földtudományi Közlemények. 2020;2020(89):336–42.
[46] Terzaghi K, Peck RB. Soil mechanics in engineering practice. New York: John Wiley & Sons; 1967.
[47] Canadian Geotechnical Society. Foundation engineering manual. Vancouver, Canada: BiTech Publishers Ltd; 1992.
[48] Labuz JF, Zang A. Mohr–Coulomb failure criterion. In: Ulusay R, editor. The ISRM suggested methods for rock characterization, testing and monitoring: 2007–2014. Cham: Springer International Publishing; 2015. p. 227–31.
[49] Fellenius W. Erdstatische Berechnungen mit Reibung und Kohäsion (Adhäsion) und unter Annahme kreiszylindrischer Gleitflächen. Berlin, Germany: W. Ernst & Sohn; 1927.
[50] Bishop AW. The use of the slip circle in the stability analysis of slopes. Geotechnique. 1955;5:7–17.
[51] Spencer E. A method of analysis of the stability of embankments assuming parallel inter-slice forces. Geotechnique. 1967;17:11–26.
[52] Janbu N. Slope stability computations. The embankment dam engineering. Casagrande volume, Editors Hirschfeld and Poulos. New York: John Wiley & Sons inc.; 1973. p. 47–86
[53] Morgenstern N, Price V. A numerical method for solving the equations of stability of general slip surfaces. Comput J. 1967;9:388–93.
[54] Crozier M. Field assessment of slope instability. In: Brunsden D, Prior D, editors. Slope instability. New York: John Wiley & Sons Ltd; 1984. p. 103–42.
[55] Zakaria Z, Sophian I, Sabila Z, Jihadi L. Slope safety factor and its relationship with angle of slope gradient to support landslide mitigation at jatinangor education area, Sumedang, West Java, Indonesia. IOP Conference Series: Earth Environ Sci. Indonesia: IOP Publishing; 2018. p. 012052.
[56] Frank R. Designers' guide to EN 1997-1 Eurocode 7: Geotechnical design-General rules. London: Thomas Telford; 2004.
[57] AASHTO LRFD Bridge Design Specifications. Washington, D.C., USA: American Association of State Highway and Transportation Officials; 2012.
[58] Das BM. Principles of geotechnical engineering. India: Thomson Learning; 2007.
[59] Hadzinakos I, Yannacopoulos D, Faltsetas C, Ziourkas K. Application of the Minora decision support system to the evaluation of landslide favourability in Greece. Eur J Oper Res. 1991;50:61–75.
[60] Lollino G, Arattano M, Cuccureddu M. The use of the automatic inclinometric system for landslide early warning: the case of Cabella Ligure (North-Western Italy). Phys Chem Earth Parts A/B/C. 2002;27:1545–50.

[61] Zayed AM, Masoud MA, Shahien MG, et al. Physical, mechanical, and radiation attenuation properties of serpentine concrete containing boric acid. Constr Build Mater. 2021;272:121641.
[62] Masoud MA, El-Khayatt AM, Kansouh WA, Sakr K, Shahien MG, Zayed AM. Insights into the effect of the mineralogical composition of serpentine aggregates on the radiation attenuation properties of their concretes. Constr Build Mater. 2020;263:120141.
[63] Zayed AM, Masoud MA, Rashad AM, et al. Influence of heavyweight aggregates on the physico-mechanical and radiation attenuation properties of serpentine-based concrete. Constr Build Mater. 2020;260:120473.
[64] Masoud MA, Kansouh WA, Shahien MG, Sakr K, Rashad AM, Zayed AM. An experimental investigation on the effects of barite/hematite on the radiation shielding properties of serpentine concretes. Prog Nucl Energy. 2020;120:103220.
[65] Hossain KA, Gencturk B. Life-cycle environmental impact assessment of reinforced concrete buildings subjected to natural hazards. J Archit Eng. 2016;22:A4014001.
[66] Hodge RA, Freeze RA. Groundwater flow systems and slope stability. Can Geotech J. 1977;14:466–76.
[67] Keqiang H, Zhiliang W, Xiaoyun M, Zengtao L. Research on the displacement response ratio of groundwater dynamic augment and its application in evaluation of the slope stability. Env Earth Sci. 2015;74:5773–91.
[68] Nguyen TS, Likitlersuang S. Reliability analysis of unsaturated soil slope stability under infiltration considering hydraulic and shear strength parameters. Bull Eng Geol Env. 2019;78:5727–43.
[69] Eab KH, Takahashi A, Likitlersuang S. Centrifuge modeling of root-reinforced soil slope subjected to rainfall infiltration. Geotech Lett. 2014;4:211–6.
[70] Bowles JE. Physical and geotechnical properties of soils. New York: McGraw-Hill Inc; 1979.
[71] Yalcin A. The effects of clay on landslides: a case study. Appl Clay Sci. 2007;38:77–85.
[72] Iqbal J, Dai F, Hong M, Tu X, Xie Q. Failure mechanism and stability analysis of an active landslide in the Xiangjiaba Reservoir Area, Southwest China. J Earth Sci. 2018;29:646–61.
[73] Binet S, Jomard H, Lebourg T, Guglielmi Y, Tric E, Bertrand C, et al. Experimental analysis of groundwater flow through a landslide slip surface using natural and artificial water chemical tracers. Hydrol Process. 2007;21:3463–72.